Journal of Advanced Research 38 (2022) 29–39

Contents lists available at ScienceDirect

Journal of Advanced Research

journal homepage: www.elsevier.com/locate/jare

High value-added application of a renewable bioresource as acaricide: Investigation the mechanism of action of scoparone against *Tetranychus cinnabarinus*

Hong Zhou [1], Fenglin Wan [1], Fuyou Guo, Jinlin Liu, Wei Ding *

Institute of Pesticide Science, College of Plant Protection, Southwest University, Chongqing 400715, PR China

HIGHLIGHTS

- Scoparone displays potent acaricidal activity against *Tetranychus cinnabarinus*.
- Scoparone modulated the Ca^{2+} signalling pathway in T. *cinnabarinus* by activating the L-type Ca^{2+} channel (L-VGCC).
- The IQ motif (a consensus CaM-binding site) of L-VGCC may be a promising novel "green acaricide"-binding target site of scoparone.

GRAPHICAL ABSTRACT

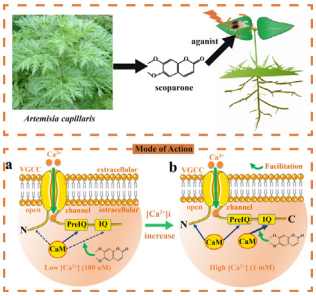

ARTICLE INFO

Article history:
Received 25 April 2021
Revised 18 August 2021
Accepted 19 August 2021
Available online 23 August 2021

Keywords:
Scoparone
Spider mites
L-type Ca^{2+} channel
Mechanism of action

ABSTRACT

Introduction: Investigation into the action mechanisms of plant secondary metabolites against pests is a vital strategy for the development of novel promising biopesticides. Scoparone (isolated from *Artemisia capillaris*), a renewable plant-derived bioresource, displays potent acaricidal activities against mites, but its targets of action remain unclear.

Objectives: This study aimed to systematically explore the potential molecular targets of scoparone against *Tetranychus cinnabarinus* and provide insights to guide the future application of scoparone as an agent for the management of agricultural mite pests worldwide.

Methods: The mechanism and potential targets of scoparone against mites were investigated using RNA-seq analysis; RNA interference (RNAi) assays; bioassays; and $[Ca^{2+}]i$, pull-down and electrophysiological recording assays.

Results: RNA-seq analysis identified Ca^{2+} signalling pathway genes, specifically 5 calmodulin (CaM1–5) genes and 1 each of L-, T-, N-type voltage-gated Ca^{2+} channel (VGCC) genes, as candidate target genes for scoparone against mites. Furthermore, RNAi and electrophysiological data showed that the CaM1- and L-VGCC-mediated Ca^{2+} signalling pathways were activated by scoparone. Interestingly, by promoting the interaction between CaM1 and the IQ motif (a consensus CaM-binding domain of L-VGCC), CaM1 markedly enhanced the activating effect of scoparone on L-VGCC. Pull-down assays further demonstrated that CaM interacted with the IQ motif, triggering L-VGCC opening. Importantly, mutation of the IQ motif significantly weakened CaM1 binding and eliminated the CaM1-mediated enhancement of scoparone-

Peer review under responsibility of Cairo University.

* Corresponding author.
E-mail address: dingw@swu.edu.cn (W. Ding).
[1] They contributed equally to this work.

https://doi.org/10.1016/j.jare.2021.08.013

induced L-VGCC activation, indicating that the effect of scoparone was dependent on the CaM1–IQ interaction.

Conclusion: This study demonstrates, for the first time, that the acaricidal compound scoparone targets the interface between CaM1 and L-VGCC and activates the CaM-binding site, located in the IQ motif at the L-VGCC C-terminus. This work may contribute to the development of target-specific green acaricidal compounds based on L-VGCC.

Introduction

The carmine spider mite, *Tetranychus cinnabarinus* (Acari: Tetranychidae), is a major agroforestry pest globally; it feeds on more than 1100 plant hosts, including tomato, peach, pepper, cotton, cucumber, citrus, strawberry, soybean, corn, apple and grape [1]. Due to its extraordinary ability to rapidly develop resistance to acaricides, this mite is considered one of the most resistant pest species and is extremely hard to prevent and control [2]. Thus, the chief strategies for battling *T. cinnabarinus* outbreaks rely on chemical acaricides; however, the increasing application of synthetic acaricides has enabled *T. cinnabarinus* to develop resistance even to newly developed acaricides within 2 years, and these chemicals exert adverse effects on humans and the environment [3,4]. Accordingly, green acaricides with novel target sites are urgently needed as potential alternatives for the effective and selective control of mite pests. Botanical bioresources originating from plant secondary metabolites are "masterpieces" of nature and have provided invaluable banks for discovering and developing novel acaricides [5,6].

Scoparone (Fig. 1a1), a well-known phenolic coumarin (Fig. 1a2), was first isolated from the Chinese herbal medicine *Artemisia capillaris* (which can be cultivated artificially, contains 4.06 mg g^{-1} in its buds and is extensively distributed in Asia), a renewable plant-derived natural bioresource (Fig. 1b) [7]. Scoparone exerts extensive pharmacological effects, such as antitumour [7], choleretic and hepatoprotective, anti-asthmatic [8], anti-allergic [9], and anti-inflammatory effects [10]. Our team recently explored the acaricidal activities of numerous natural coumarin derivatives against *T. cinnabarinus* [11,12] and found that scoparone, one of the most potent natural products (Fig. S1), exhibits potent acaricidal activity against the mites [13].

Many reports have been published about the acaricidal activities of natural products against different pests [12,14], and a few studies have focused on the underlying mechanisms. In previous studies, exposure to scoparone has been found to cause several typical signs of nerve agent exposure, such as excitement, convulsion and paralysis [13]. Considering that Ca^{2+} is an intracellular second messenger that controls muscle contraction, scoparone might disrupt Ca^{2+} homeostasis, resulting in flaccid paralysis of *T. cinnabarinus* [15,16]. Recently, studies have reported that only novel diamide insecticides, including the world's top-selling insecticides (such as flubendiamide and chlorantraniliprole), can act primarily on the muscular system and activate intracellular Ca^{2+} release and ryanodine receptors (RyRs) [17,18]. However, unlike the molecular mechanisms of diamide insecticides, the potential acaricidal mechanism of scopoletin (6-methoxy-7-hydroxycoumarin), a structural analogue of scoparone, is associated with the activation of the L-type voltage-gated Ca^{2+} channel (L-VGCC) [19,20].

Ca^{2+} is a key signalling molecule in neurons that regulates various biological processes, such as muscle contraction, gene expression, and neurotransmitter release [21]. Normally, intracellular Ca^{2+} levels are maintained in a balanced state known as Ca^{2+} homeostasis [22]. The regulation of Ca^{2+} homeostasis is mediated by channels and receptors, such as voltage-gated Ca^{2+} channels (VGCCs) [23], Ca^{2+} pumps [24], RyRs [17], calmodulin (CaM) [25], and inositol triphosphate receptor (IP_3R) [26], which may be targets of acaricide/insecticide action. It has been reported that scoparone induces neurite outgrowth in rat adrenal pheochromocytoma (PC12) cells by activating Ca^{2+}/CaM kinase II- and protein kinase A- and C-mediated Ca^{2+} influx, implying that intracellular Ca^{2+} signalling may be activated by scoparone [27]. Recently, several studies have indicated that L-VGCC is the primary target through which coumarin derivatives control mite pests [19,20].

VGCCs play a principal role in neurological function and are indispensable for transforming electrical signals into biochemical events [23]. Neurons express multiple VGCCs with different physiological functions, including the L-, N-, P-, Q-, R-, and T-type channels [19]. L-VGCC plays key roles in survival, learning and other adaptive responses in neurons [23]. The activity of L-VGCC is reverse-modulated by intracellular Ca^{2+}, which is mediated by CaM. CaM interacts with L-VGCC, resulting in both Ca^{2+}-dependent facilitation (CDF) and Ca^{2+}-dependent inactivation (CDI) [28]. To date, how CaM interacts with L-VGCC to induce CDF and CDI remains unclear. Several regions of L-VGCC, including N-terminal (NT) and C-terminal (CT) regions such as the EF-hand, Pre-IQ and IQ regions, have been shown to play roles in mediating CDF and CDI. The IQ region is widely accepted as a CaM-binding site [29]. Ca^{2+} signalling mediated by L-VGCC and CaM is known to be targeted by numerous natural small molecules, including insecticides and drugs for arrhythmias and nervous disorders [17,29]. To the best of our knowledge, this is the first study to explore a renewable natural acaricidal agent targeting the Ca^{2+} signalling pathways of mite pests.

Materials and methods

Ethics statement

This article does not contain any studies with human or animal subjects.

Mites

Tetranychus cinnabarinus specimens were originally collected from *Vigna unguiculata* seedlings in Beibei, Chongqing, China, in June 2002 and then maintained without exposure to any xenobiotics at 26 ± 1 °C and 70%~75% relative humidity under a 14 h/10 h light/dark cycle [20,30].

RNA-seq analysis

Total RNA of mites was extracted with TRIzol (Tiangen, Beijing, China) following the manufacturer's instructions and then used to construct mRNA sequencing libraries. An Ion Proton platform (BGISEQ-500 platform, BGI, Shenzhen, China) was used to perform RNA-seq and analysis. Bowtie2 was used to obtain high-quality reads by aligning the reads against the reference genome of the sister species *T. urticae*. RNA-seq by Expectation-Maximization

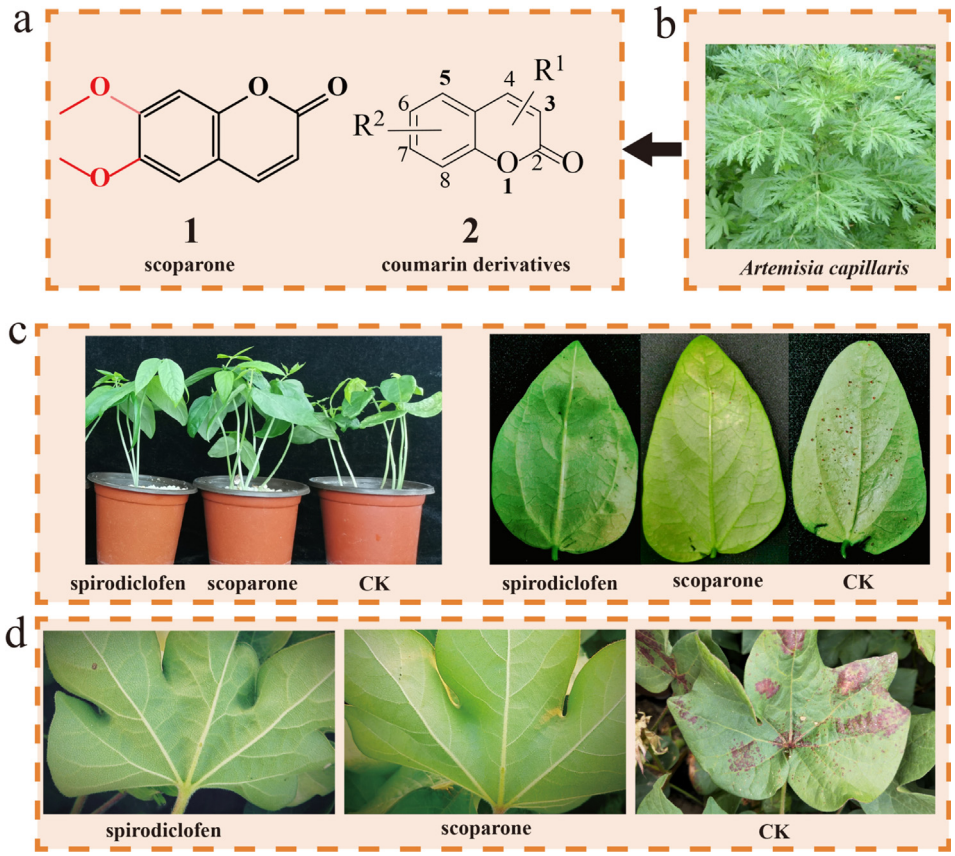

Fig. 1. Chemical structures of scoparone (1) and its derivatives (2), and representative images of the control efficiency achieved with scoparone. a, b Isolation of scoparone (1) and its derivatives (2) from *A. capillaris*. c, d Representative images of the control efficiency of scoparone and spirodiclofen (a positive control) against *T. cinnabarinus* in greenhouse (c) and field (d) tests.

(RSEM) was used to normalize the expression level of each gene in the RNA-seq data to the fragments per kilobase of exon model per million mapped reads (FPKM) value. To confirm the RNA-seq results, qRT-PCR analysis of 15 randomly selected significantly differentially expressed genes was performed. Principal component analysis (PCA) was then performed to further confirm the RNA-seq results. Functional enrichment analysis was performed by mapping the genes with the Gene Ontology (GO) and Kyoto Encyclopedia of Genes and Genomes (KEGG) databases. The Search Tool for the Retrieval of Interacting Genes/Proteins (STRING) was then employed to construct a protein–protein interaction (PPI) network based on the candidate target genes.

Bioassay

The Food and Agriculture Organization (FAO)-recommended slip-dip method was used to detect the toxicity of compounds against mites as described previously [13], and the sublethal concentrations (LC_{30}, LC_{50} and LC_{70}) against mites were determined through a log-probit analysis of bioassay data using IBM SPSS Statistics (v.16.0, Chicago, IL, USA).

$[Ca^{2+}]i$ assay

Spodoptera frugiperda cells (Sf9, Invitrogen, Carlsbad, CA, USA) were cultivated at 27 ± 1 °C in 15 mL of Sf-900™ SFM culture medium (Gibco, CA, USA). Fluo-4/AM fluorescence staining was performed to determine the $[Ca^{2+}]i$ of the cells as described previously [20].

CaM activity and cytotoxicity assays

The activity of the CaM protein was assayed as the ability of the protein to activate phosphodiesterase (PDE) (Sigma, St. Louis, MO, USA), which hydrolyses cAMP (Sigma) to 5′-AMP [30]. Then, 5′-AMP was broken down into adenosine and orthophosphate (Pi) by 5′-nucleotidase (Sigma), which was measured using spectrophotometry at 660 nm. An MTT Cell Proliferation and Cytotoxicity Assay Kit (Solarbio, Shanghai, China) were used to determine the cytotoxicity of the compound following the manufacturer's protocol [31]. The median lethal concentration (LC_{50}) for the assay was analysed with IBM SPSS Statistics (v.16.0).

Heterologous expression

The *Bac*-to-*Bac* baculovirus system (Invitrogen) was used to express CaM1 in Sf9 cells following the manufacturer's protocol [31]. Briefly, the coding motif of the CaM1 gene was ligated into the expression vector (pFastBac HTA), which was then transfected into Sf9 cells. After cultivation for 3 d at 27 °C, CaM1-expressing Sf9 cells were collected and further resuspended to measure the specific activation of PDE by CaM1.

PCR assay

Specific primers (Table S1) were designed and synthesized to obtain the DNA sequences of genes based on the complete genome of the sister species *T. urticae*. RT-PCR and qRT-PCR analyses were performed using a rTaq™ Polymerase Kit (Takara, Dalian, China) and an iQ™ SYBR® Green Supermix Kit (Bio-Rad, Hercules, CA,

USA), respectively, as described previously [20]. *RPS18* was used as the reference gene (Table S1).

RNA interference (RNAi) analysis

A Transcriptaid T7 High Yield Transcription Kit (Thermo Scientific, Lithuania, EU) was used to synthesize dsRNAs following the manufacturer's instructions. A leaf disc-mediated dsRNA feeding method was employed to knock down target gene expression as described in our previous study [20]. The GFP gene (ACY56286) was treated as a negative control.

Plasmid construction

All the primers used for plasmid construction are listed in Table S1. A glutathione S-transferase (GST)-tagged CaM1 construct was generated by cloning a PCR product encoding CaM1 into the expression vector pGEX-6P-1. The L-VGCC constructs for the Ca^{2+} channel activity analyses were generated by cloning PCR products encoding the amplified cDNAs into the expression vector pT7T. Eight GST-tagged constructs encoding L-VGCC cytoplasmic regions were obtained by subcloning the PCR products encoding full-length L-VGCC and inserted into the expression vector pGEX-6P-1 as GST-fusion peptides. The plasmid constructs for all experiments were verified by DNA sequencing.

Expression and purification of GST-fusion peptides

The plasmids encoding CaM1 and L-VGCC truncation mutants were transformed into *Escherichia coli* BL21(*DE3*) competent cells, which were then cultivated with 0.1 mM isopropyl β-D-1-thiogalactopyranoside (IPTG) (Solarbio) for 24 h at 37 °C. The fusion proteins were purified with BeyoGold™ GST-tag Purification Resin (Beyotime Biotechnology, Beijing, China) following the manufacturer's protocol. The purified yields were analysed via SDS-PAGE and further determined using the Bradford method [32].

GST pull-down assay

A Pierce™ GST Protein Interaction Pull-Down Kit (Thermo Scientific) was used to perform GST pull-down assays according to the manufacturer's instructions. Briefly, the purified CaM1 protein was cultivated with GST-tagged truncated L-VGCC protein or GST protein alone (CK, Sigma) in buffer (25 mM Tris-HCl, 0.15 M NaCl, pH 7.2) using glutathione agarose beads at 4 °C for 24 h. The incubated proteins were washed, resuspended in 4X SDS-PAGE loading buffer (Takara) at 50 °C for 5 min, and then separated with a 12% SDS-PAGE gel. Coomassie Brilliant Blue R staining was conducted to visualize the proteins. The protein contents were analysed using Photoshop software (Adobe, San Jose, CA) [32].

Electrophysiological recording

Xenopus oocytes were used to express the *TcL-VGCC* gene, and the whole-cell currents were recorded using electrode voltage-clamp following the methods described in previous works [33]. Data acquisition and analysis were performed using Digidata 1440A and pCLAMP 10.2 software (Axon Instruments, Inc., CA, USA) [34]. Dose-response curves for the assay were analysed using IBM SPSS Statistics (v.16.0).

Experimental design and treatments

To explore the candidate targets of scoparone, RNA-seq analysis was performed to examine the transcription level changes in mites exposed to the LC_{50} dose of scoparone. Their cDNA sequences were cloned and then characterized to further explore the molecular functions of the CaM- and VGCC-mediated Ca^{2+} signalling pathway-related genes. Subsequently, a phylogenetic analysis was performed with MEGA 5.0 based on the known amino acid sequences of *TcVGCCs* and *TcCaMs* with orthologues from arachnids, mammals and insects. The expression levels of *TcVGCCs* and *TuVGCCs* at different life stages (egg, larva, nymph, and female adult) were then evaluated via qRT-PCR and RT-PCR. To verify whether scoparone activates the expression of VGCCs and CaM-mediated Ca^{2+} signalling pathway-related genes at the 30% lethal concentration (LC_{30}), LC_{50}, and 70% lethal concentration (LC_{70}) doses, qRT-PCR and RT-PCR analyses were performed after scoparone treatment.

To investigate how CaM1 binds to the NT or CT motif of L-VGCC to regulate CDF and CDI, GST-fusion peptides of the L-VGCC NT motif and three CT motifs, including near-end (CT1), middle (CT2), and distal (CT3) motifs, were prepared. For the CT1 motif, which features key modulation domains including the EF-hand motif (Ca^{2+}-binding domain, EF) and two CaM-binding motifs (PreIQ and IQ), four CT1 constructs were produced: CT1A (EF and PreIQ), CT1B (PreIQ and IQ), PreIQ, and IQ. Subsequently, to test whether CaM binding to the IQ motif is required for scoparone to overactivate Ca^{2+} signalling mediated by inhibition of CDI or promotion of CDF of L-VGCC, point mutants with mutations that specifically disrupted CaM binding to this region were generated.

Statistical analysis

The data from all experiments were analysed with the Student's *t*-test to assess the statistical significance of differences between two groups. Differences in all tests were deemed significant when $p < 0.05$.

Data availability

The RNA-seq data presented in this article have been deposited in the Sequence Read Archive (SRA) with accession number PRJNA596823.

Results

Biological activity of scoparone

Bioassay experiments showed that scoparone exhibited more potent acaricidal activity against *T. cinnabarinus* than the commercial acaricide spirodiclofen in greenhouse and field trials (Fig. 1c-d; Table S2). Additionally, scoparone exhibited significant acute toxicity towards pests, including spider mites (*T. cinnabarinus*, *T. urticae*, and *Panonychus citri*) and *Aphis gossypii*; in contrast, it showed no toxicity towards nontargeted beneficial organisms, such as the predatory mite *Neoseiulus barkeri*, honey bees (*Apis mellifera*), and silkworms (*Bombyx mori*) (Table S3; Fig. S2), indicating that scoparone may be useful as a highly selective green/eco-friendly botanical acaricidal agent to control mite pests.

RNA-seq analysis

RNA-seq analysis demonstrated that 251 genes were significantly differentially expressed in the scoparone group compared with the control (CK) group, 192 of which were upregulated and 59 of which were downregulated (Fig. 2a-c; Table S4–5; Fig. S3). qRT-PCR analysis indicated that all tested differentially expressed genes exhibited expression trends consistent with the RNA-seq data (Fig. 2d). Subsequently, PCA revealed that the scoparone and control groups had similar gene expression clusters (Fig. S4).

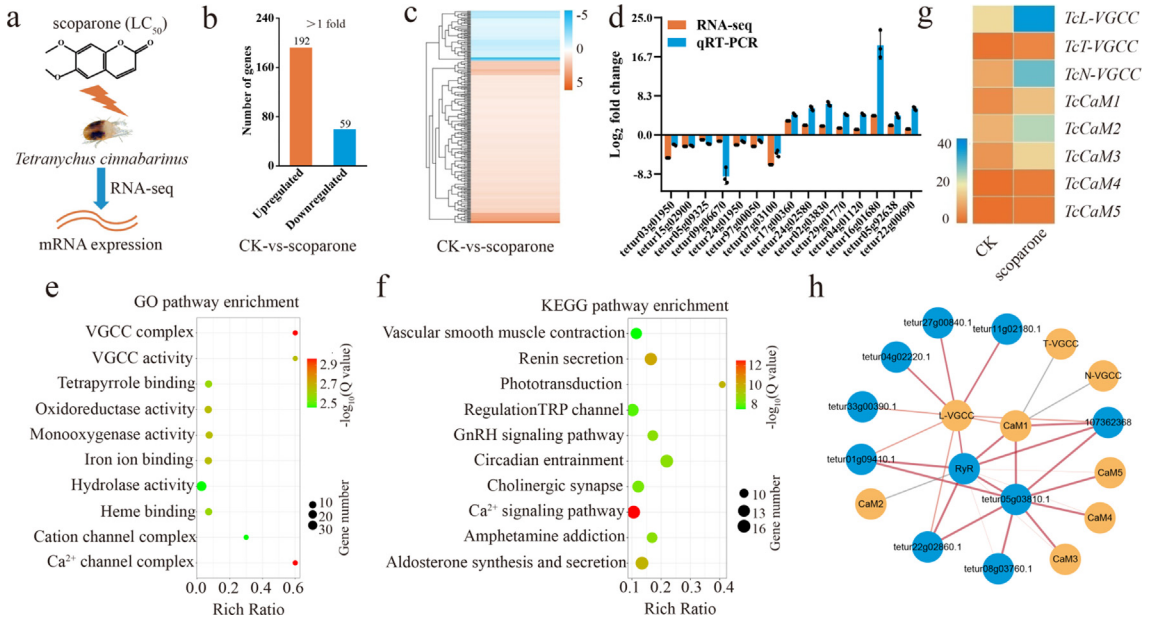

Fig. 2. RNA-seq analysis revealed candidate targets for scoparone against *T. cinnabarinus*. a Diagram of the candidate targets for scoparone against mites as determined by RNA-seq. b Distributions of the differentially expressed genes in *T. cinnabarinus* in response to scoparone. c Heat map of significantly differentially expressed genes in the scoparone group vs the control group. d qRT-PCR validation of 15 differentially expressed genes identified by RNA-seq. e, f Top 10 enriched GO (e) and KEGG (f) pathways of the differentially expressed genes. The "rich ratio" is defined as the ratio of the number of differentially expressed genes enriched in the pathway to the total number of genes enriched in the same pathway. g Heat map of the candidate target genes involved in the Ca^{2+} signalling pathway. h PPI network generated from a STRING analysis. The size and colour depth of each straight line are positively correlated with the degree of connectedness with other proteins.

The top 10 GO terms included the "VGCC complex", "calcium channel complex", "monooxygenase activity", and "VGCC activity" terms, among others (Fig. 2e). The top 10 KEGG terms included the "calcium signalling pathway", "renin secretion", "phototransduction", and "aldosterone synthesis and secretion" terms (Fig. 2f). Among the top 10 terms from the GO and KEGG analyses, the most highly enriched terms were "VGCC complex" and "calcium signalling pathway", respectively. Next, 1 l-VGCC (*TcL-VGCC*), 1 T-type VGCC (*TcT-VGCC*), 1 N-type VGCC (*TcN-VGCC*), and 5 CaM (*TcCaM1–5*) genes associated with the "calcium signalling pathway" term were selected as candidate target genes for further investigation (Fig. 2g). The PPI network showed that CaM1 is the primary relevant signalling molecule for L-, T-, and N-VGCCs (Fig. 2h).

CaM1- and L-VGCC-mediated Ca^{2+} signalling pathways were essential for the acaricidal mechanism of scoparone

The sequence alignment results showed that the *TcVGCCs* have four functional regions (domains I-IV), each of which consists of 6 transmembrane α-helix segments (S1-S6) (Fig. 3a; Table S6; Fig. S5). Additionally, *TcCaM1* and *TcCaM5* include 4 and 2 EF-hand domains, respectively, and *TcCaM3* contains 1 transmembrane helix (Fig. 3b; Fig. S6). Next, phylogenetic analysis showed that *TcVGCCs* and *TcCaMs* share the highest sequence similarity with VGCCs and CaMs of *T. urticae*, respectively, indicating evolutionary relatedness and potential homologous physiological mechanisms between *TcVGCCs* and *TuVGCCs* and between *TcCaMs* and *TuCaMs* (Fig. S7–8; Table S7). qRT-PCR and RT-PCR analyses showed that *TcVGCCs* and *TcCaMs* were expressed throughout all developmental stages, demonstrating that *TcVGCCs* and *TcCaMs* are involved in all bioprocesses of development and growth (Fig. S9).

Next, qRT-PCR and RT-PCR analyses indicated that the expression of VGCC and CaM genes was upregulated in the scoparone exposure groups compared with the control group at 48 h post-treatment (Fig. S10). In addition, scoparone upregulated the expression levels of the L-VGCC and CaM1 genes more significantly than other Ca^{2+} signalling pathway-related genes. RNAi analysis indicated that the transcript levels of L-, T-, N-VGCC, and CaM1–5 were significantly lower (50–72% lower) in mites fed the separate corresponding candidate dsRNA for 48 h than in control mites, suggesting that RNAi successfully silenced the transcription of *TcVGCCs* and *TcCaMs* in the mites (Fig. 3c-e; Fig. S11). Moreover, RNAi of L-VGCC and CaM1 markedly knocked down the transcription of these candidate genes simultaneously (by 68% and 60%, respectively) (Fig. 3e). Next, the susceptibility of mites to scoparone after RNAi of *TcVGCCs* and *TcCaMs* was analysed. Mortality was significantly lower for the mites in which the *TcL-VGCC* and *TcCaM1* genes were individually silenced than for the control mites (Fig. 3f; Table S8). Interestingly, *TcL-VGCC*- and *TcCaM1*-targeting dsRNA provided the largest decreases in mortality (7.25- and 5.50-fold, respectively), and silencing the L-VGCC and CaM1 genes simultaneously had a more powerful effect on mortality (measured as a fold change; 11.43-fold greater) in mites than knocking down the single genes (Table S8). Together, these results indicated that the CaM1- and L-VGCC-mediated Ca^{2+} signalling pathways were essential for the acaricidal mechanism of scoparone.

CaM1- and L-VGCC-mediated Ca^{2+} signalling pathways were activated by scoparone

The activity of CaM1 was verified with a PDE activation assay. The activity of purified CaM1 (284.1 nmol mg^{-1} min^{-1}) was almost 3.11 times higher than that of crude protein extracted from mites (91.3 nmol mg^{-1} min^{-1}) (Table S9). Typically, assessing the efficacy of an acaricide against mite pests depends mainly on measurement of typical acute toxicity represented by the median lethal concentration or dose (LC_{50}) [30]. However, the EC_{50}, the half-maximal effective concentration, is a representative indicator of the effect of interactions between small molecule drugs and target proteins [33]. In this study, the EC_{50} of scoparone for PDE activation by

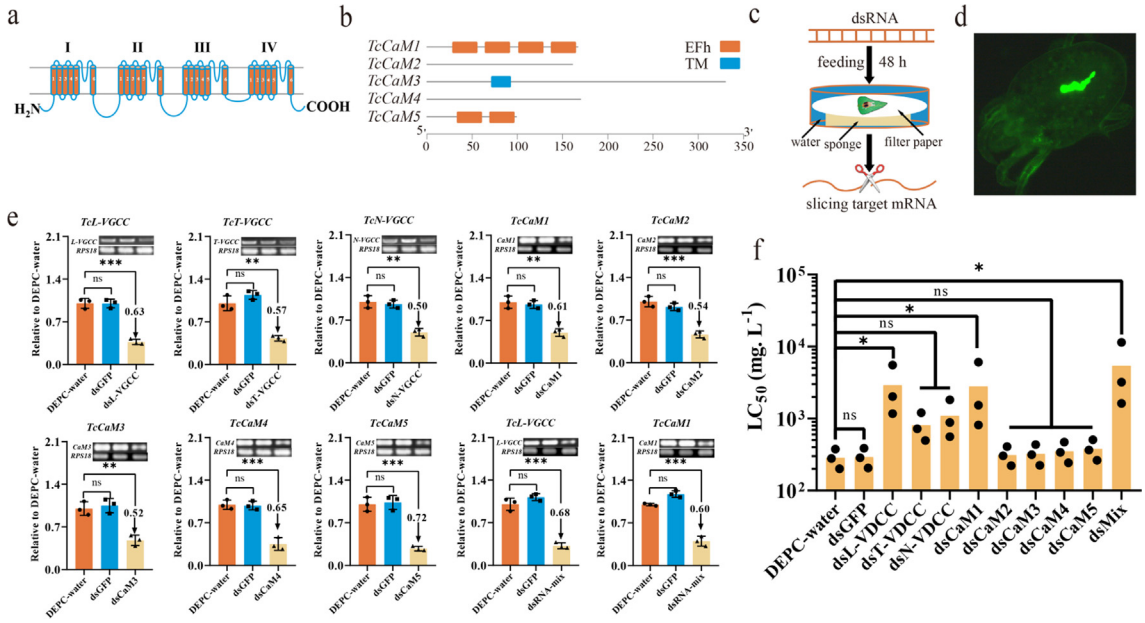

Fig. 3. CaM1- and L-VGCC-mediated Ca^{2+} signalling pathways were essential for the acaricidal mechanism of scoparone. a, b Schematic drawing of VGCCs (a) and CaMs (b). COOH, CT region; NH_2, NT region; 1–6 and TM, transmembrane helices; I-IV, domains I-IV; EFh, EF-hand domains. c Schematic drawing of leaf disc-mediated RNAi in mites. d dsRNA was successfully delivered to target tissues in mites by leaf disc-mediated RNAi. dsGFP was labelled with FAM (6-carboxy-fluorescein). Positive staining for dsGFP is shown as green zones in the images captured under a microscope. e qRT-PCR and RT-PCR analyses of *TcVGCC* and *TcCaM* expression after RNAi at 48 h post dsRNA feeding relative to the expression after DEPC-water treatment, respectively. f Summary of the LC_{50} values after RNAi. The data are shown as the mean ± SD from three independent experiments. $^{*}p < 0.05$, $^{**}p < 0.01$, $^{***}p < 0.001$. ns, not significant.

CaM1 was 4.92 μM, suggesting that scoparone could indirectly activate the CaM1 protein *in vitro* (Fig. 4a-c). Additionally, the CaM1 assay showed that compared with the control treatment, treatment with the LC_{70}, LC_{50}, and LC_{30} doses of scoparone for 48 h markedly increased the specific activation of PDE by extracted CaM *in vivo* (by 3.67-, 2.79-, and 1.87-fold, respectively), further demonstrating that scoparone is an agonist of CaM1 (Fig. 4d). Next, mites were fed a specific inhibitor of CaM, trifluoperazine (TFP), to further confirm the findings. A toxicity assay indicated that the LC_{50} of scoparone in mites in which endogenous CaM1 was blocked by pretreatment with the half-maximal inhibitory concentration (IC_{50}) of TFP (Fig. 4e) was 3.27-fold higher (Table S8) than that in control mites, suggesting that the mechanism of action of scoparone against mites is mediated by activation of CaM1.

Ca^{2+} signalling in cells can be mediated by increased CaM activity [25]. Thus, an intracellular [Ca^{2+}]i assay was performed to investigate [Ca^{2+}]i in scoparone-treated cells. The [Ca^{2+}]i in Sf9 cells was markedly increased after scoparone exposure in a dose-dependent manner, whereas it was dramatically reduced in TFP-pretreated Sf9 cells, suggesting that CaM1 was involved in [Ca^{2+}]i overload in scoparone-treated cells (Fig. 4f-g). Furthermore, functional CaM1 was expressed in Sf9 cells *in vitro* to further confirm our findings. A CaM assay demonstrated that CaM-specific activity in CaM1-expressing cells was 15.56-fold higher than that in GFP-expressing cells (Fig. 4h-i). In addition, a [Ca^{2+}]i assay revealed that [Ca^{2+}]i in CaM1-expressing cells treated with scoparone dramatically exceeded that in GFP-expressing cells (Fig. 4j). Subsequently, a cytotoxicity assay was performed to detect the toxicity of scoparone against CaM1- or GFP-expressing Sf9 cells, the results of which indicated that CaM enhanced the toxicity of scoparone in Sf9 cells (Fig. 4k; Table S10). These findings indicated that CaM1-mediated Ca^{2+} signalling pathways in mites were activated by scoparone.

Electrophysiological experiments demonstrated that in the absence of CaM1, scoparone significantly increased the current, with an EC_{50} value of 5.54 μM, in oocytes expressing L-VGCC alone (Fig. 4l and 4n; Table S11; Fig. S12). In contrast, the EC_{50} value of scoparone in oocytes expressing L-VGCC and pretreated with CaM1 (at a K_{df} of 0.61 μM) was reduced ~ 10-fold to 0.46 μM (Fig. 4-m-n; Table S11), indicating that CaM1 enhanced the Ca^{2+} channel-activating effect of scoparone. Next, the concentration-dependent effects of CaM1 were investigated to further confirm our findings. CaM1 showed a clear bell-shaped activity curve: at relatively low concentrations, it promoted channel opening, but at higher concentrations, it inhibited channel activity (Fig. 4o and 4q). The dose-dependent effect of CaM1 on L-VGCC activity was further measured in the presence of 5.54 μM scoparone (Fig. 4p-q). The facilitating effect of CaM1 was significantly enhanced (the K_{df} value was reduced from 0.61 to 0.28), but the inhibitory effect was significantly decreased (the K_{ni} value was increased from 8 to 12) (Fig. 4q; Table S12), indicating that activation of CaM1 and L-VGCC by scoparone likely induced excessive activation of Ca^{2+} signalling pathways by promoting CDF or blocking CDI of L-VGCC.

CaM1 was able to bind to the NT and CT peptides of L-VGCC

The activity of L-VGCC is modulated by CDF and CDI [28]. CaM has been proven to be a Ca^{2+} transducer that induces Ca^{2+}-dependent conformational changes in the L-VGCC protein to mediate CDF and CDI [29]. Pull-down assays demonstrated that CaM1 was markedly bound to the NT, CT1, CT1B, PreIQ, and IQ peptides, whereas its binding to CT2, CT3, and CT1A was negligible (Fig. 5a-d). These findings indicated that CaM1 bound to both the NT and proximal CT motifs of L-VGCC. The stoichiometry of CaM1 binding with five peptides under two [Ca^{2+}]I conditions, 100 nM (resting [Ca^{2+}]i) and 1 mM (saturating [Ca^{2+}]i), was then analysed. Under 1 mM Ca^{2+}, CaM1 binding to CT1 and CT1B was best fitted with a two-site model (Fig. 5e-f; Table S13), implying that more than one molecule of CaM1 bound to the CT motif. The curve-fitting analysis suggested that the ranking of the K_d values was CT1B < CT1 = IQ < PreIQ < NT. Under 100 nM Ca^{2+}, the ranking of the K_d values was similarly evaluated, and the order was as fol-

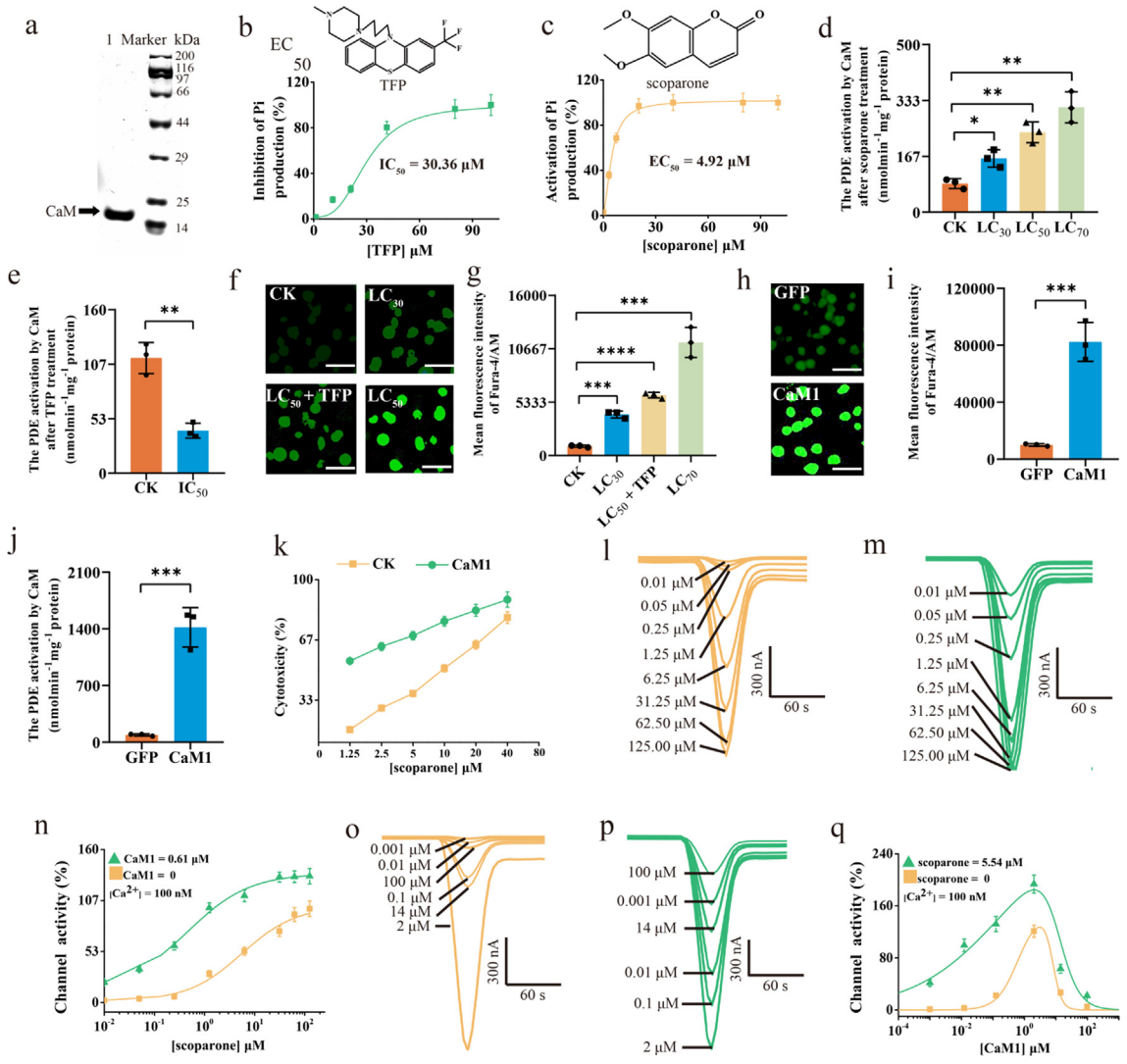

Fig. 4. CaM1 and L-VGCC-mediated Ca^{2+} signalling pathways were activated by scoparone. a Expression of recombinant CaM1 protein (lane 1) by *E. coli*. b, c IC_{50} of TFP (b) and EC_{50} of scoparone (c) as determined by CaM1 protein assay. d, e The specific activation of CaM in *T. cinnabarinus* exposed to scoparone (d) and 30.4 μM TFP (IC_{50}, e) was determined. f, g Effects of scoparone on intracellular free Ca^{2+} levels ($[Ca^{2+}]i$) in Sf9 cells. Positive staining for Ca^{2+} is shown as green zones in the images captured under a microscope. 'LC_{50} + TFP' indicates TFP-pretreated (IC_{50} dose of TFP) Sf9 cells incubated with 0.28 mg/mL scoparone for 48 h. h, i $[Ca^{2+}]i$ of GFP- and CaM-expressing cells exposed to 0.28 mg/mL scoparone for 48 h. j Specific induction of PDE activity against the substrate cAMP by recombinant CaM1 expressed by *E. coli*. k Cytotoxicity of scoparone towards CaM- and GFP-expressing cells; scale bar = 40 μm. l, m, n Representative whole-cell responses to L-VGCC agonism and channel activity were induced by scoparone in non-pretreated cells (l, n) and cells pretreated with 0.61 μM CaM1 (K_{df} dose of CaM1) (m, n). o, p, q Representative whole-cell responses to L-VGCC agonism and channel activity were induced by CaM1 in non-pretreated cells (o, q) and cells pretreated with 5.54 μM scoparone (EC_{50} dose of scoparone) (p, q). The data are shown as the mean ± SD from three independent experiments. $^{*}p < 0.05$, $^{**}p < 0.01$, $^{***}p < 0.001$, $^{****}p < 0.0001$.

lows: PreIQ < NT < CT1B < CT1 < IQ (Fig. 5g-h; Table S13). These results support the hypothesis of Ca^{2+}/CaM-mediated modulation of L-VGCC. At low $[Ca^{2+}]i$, CaM exists mainly as a Ca^{2+}-free form (apoCaM) and interacts preferentially with PreIQ (a CT motif of the Ca^{2+} channel), producing basal channel activity. However, when $[Ca^{2+}]i$ increases, Ca^{2+} binds with CaM, forming Ca^{2+}/CaM, which interacts preferentially with the IQ motif, triggering CDF. A further increase in $[Ca^{2+}]i$ enhances the binding of Ca^{2+}/CaM with PreIQ/NT, leading to CDI.

Scoparone facilitated CaM1 binding to the IQ domain of L-VGCC

In the absence or presence of scoparone (EC_{50}, 5.54 μM), a pull-down assay was performed to compare the binding of CaM1 (K_{df}, 0.61 μM) to peptides such as NT, CT1, CT1B, PreIQ, and IQ under 1 mM Ca^{2+}. Although CaM1 binding to the NT region and PreIQ tended to be decreased, while binding to CT1 and CT1B tended to be only slightly increased, CaM1 binding to the IQ domain was markedly increased in the presence of scoparone (47.06%, Fig. 6a-b). The effects of scoparone on the binding of IQ, PreIQ, and NT peptides under different CaM1 concentrations were further analysed. Scoparone markedly left-shifted the binding of CaM1 to the IQ peptide under 1 mM Ca^{2+} (Fig. 6c-d), changing the K_{df} value of CaM from 0.43 to 0.23 μM (Table S13). These findings indicated that CaM1 and scoparone together activated the IQ peptide. Similar experiments under 100 nM Ca^{2+} were further performed and obtained essentially the same results (Fig. 6c and 6e). However, CaM1 binding to the PreIQ and NT peptides was not markedly affected by scoparone at total CaM1 concentrations greater than 1 μM under 1 mM Ca^{2+} (Fig. S13). CaM1 binding to PreIQ and NT peptides tended to be shifted rightward by scoparone under 1 mM Ca^{2+} (Fig. S13). It was difficult to examine the effect of scoparone on the binding of the PreIQ and NT motifs with CaM1 under 100 nM Ca^{2+} by pull-down assay because of low affinity between

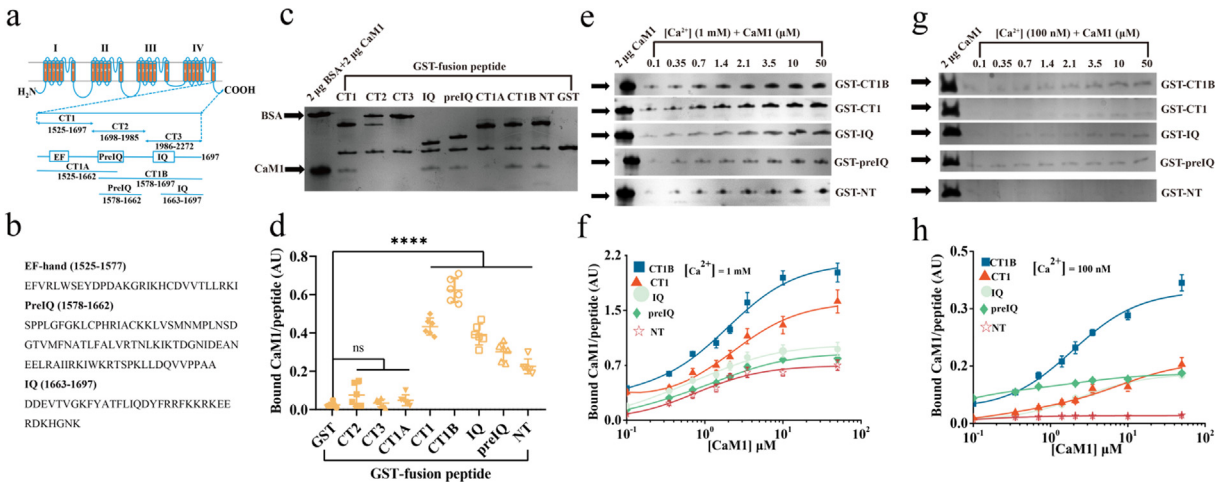

Fig. 5. CaM1 could bind to the NT and CT peptides of L-VGCC. a Schematic drawing of peptide fragments of L-VGCC. Eight peptides derived from the intracellular regions of the channel, including CT and NT peptides, were constructed as GST-fusion peptides. The CT domain was divided into three parts, as illustrated. CT1 contained regulatory regions (shown as boxes), a Ca^{2+}-binding EF-hand motif (EF), and two CaM-binding domains (PreIQ and IQ). Fragments of CT1 (i.e., CT1A, CT1B, PreIQ, and IQ) were also prepared. b Amino acid sequence deduced from the EF-hand, PreIQ and IQ domains. c, d GST pull-down assay for CaM binding under 1 mM Ca^{2+}. GST-fusion peptides (0.35 μM) were mixed with 0.35 μM CaM1, and bound CaM1 was separated by SDS-PAGE. Two micrograms of BSA (66 kDa) and 2 μg of CaM1 (19 kDa) were run as standards. e-h Concentration-dependent binding of CaM1 to CT1 (△), CT1B (□), IQ (○), PreIQ (◇), and the NT region (☆) under 1 mM Ca^{2+} (e, f) and 100 nM Ca^{2+} (g, h). The data are shown as the mean ± SD from six independent experiments. $^{****}p < 0.0001$. ns, not significant.

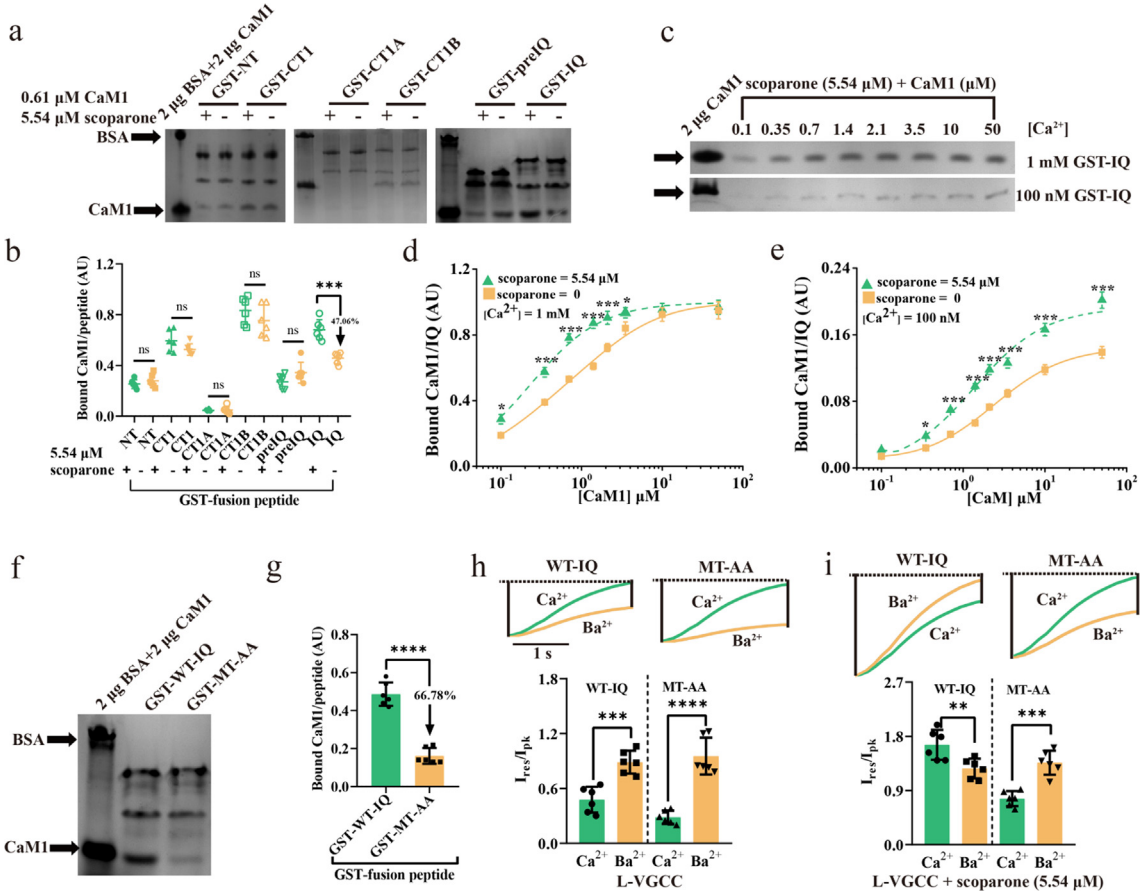

Fig. 6. Scoparone facilitated CaM1 binding to the IQ domain of L-VGCC. a GST pull-down assay for CaM1 (K_{df}, 0.61 μM) binding to peptides (NT, CT1, CT1A, CT1B, PreIQ, and IQ peptides) under 1 mM Ca^{2+}. CaM1 binding was examined in the presence of scoparone (EC_{50}, 5.54 μM). BSA (2 μg) and CaM1 (2 μg) were run as standards. b Summary of CaM1 binding by scoparone under 1 mM Ca^{2+}. c-e Dose-dependent binding of CaM1 to IQ under 1 mM Ca^{2+} (c, d) and 100 nM Ca^{2+} (c, e) in the presence of 5.54 μM scoparone. For comparison, curves of CaM1 binding in the absence of scoparone were taken from Fig. 5 or constructed, and the fitted curves were superimposed as solid lines. f, g GST fusion peptides (WT-IQ, MT-AA, 0.61 μM) were mixed with 0.61 μM CaM1. h Representative recorded currents and the residual fractions of peak currents (I_{res}/I_{pk}) from L-VGCC (WT-IQ) and its mutants (MT-AA) during test pulses of V_h from −80 to + 40 mV. I_{Ca} was scaled to the peak I_{Ba}. i Representative recorded currents and I_{res}/I_{pk} from L-VGCC (WT-IQ) and its mutants (MT-AA) after pretreatment with 5.54 μM scoparone during test pulses of V_h from −80 to + 40 mV. The I_{res}/I_{pk} remaining at the end of a 2-s test pulse was plotted for I_{Ca} and I_{Ba} supported by WT-IQ and MT-AA. The data are shown as the mean ± SD from six independent experiments. $^{*}p < 0.05$, $^{**}p < 0.01$, $^{***}p < 0.001$, $^{****}p < 0.0001$. ns, not significant.

PreIQ and CaM1 and between the NT motif and CaM1. Overall, these results demonstrated that scoparone facilitated CaM1 binding to the IQ domain of L-VGCC.

Given that Ile and Gln are the key consensus amino acid residues in the CaM-binding IQ motif in wild-type-IQ (WT-IQ) L-VGCC and that mutant-IQ (MT-IQ) L-VGCC has profoundly altered Ca^{2+}-sensitive feedback mechanisms [35], the two key positions (Ile and Gln) in the L-VGCC IQ motif were then simultaneously replaced with Ala (Fig. S14 and S15). The binding of CaM1 to GST fusion peptides with wild-type and mutant IQ motifs (GST-WT-IQ and GST-MT-AA, respectively) was first investigated. Pull-down assays demonstrated that, compared with the peptide with the WT-IQ motif (GST-WT-IQ), the peptide with mutation of the IQ domain (GST-MT-AA) exhibited significantly weaker CaM1 binding (66.78%; Fig. 6f-g).

The effects of WT-IQ L-VGCC and MT-IQ (MT-AA) L-VGCC on inactivation or facilitation during sustained depolarization were then assessed. To directly compare regulation by CaM in these experiments, Ca^{2+} currents (I_{Ca}s) were restricted to analysis, as Ba^{2+} currents (I_{Ba}s) show no CaM-dependent enhancement of inactivation or facilitation [36]. I_{Ca} and I_{Ba} were recorded in the same oocytes to characterize the effects of Ca^{2+} entry on the decline in current during a standard depolarizing pulse to + 40 mV. In oocytes expressing L-VGCC, I_{Ca} decayed almost completely during the 2-s pulse due to CDI mediated by endogenous CaM in these oocytes, indicating that CDI was prominent with the WT-IQ channel (Fig. 6h). Although the MT-AA channels were weakly bound to CaM1, CDI was still evident in these channels, as inactivation of I_{Ba} was significantly lower than that of I_{Ca} in oocytes. Compared with those of the WT-IQ L-VGCC, the value of *I* for the MT-AA channel was 2.72-fold higher (2.35 vs. 0.86), and the value of *F* for the MT-AA channel was 1.51-fold lower (-0.70 vs. −0.46) (Fig. S16). These findings indicated that a mutation of the IQ motif that significantly weakened CaM binding promoted CDI and blocked CDF of the Ca^{2+} channel.

The residual CaM-mediated regulation of MT-AA channels suggested that CaM-IQ interactions actively suppressed inactivation or promoted facilitation of I_{Ca}. If so, then scoparone should not block CDI or promote CDF in MT-AA channels because scoparone should enhance CaM binding to the IQ motif of the Ca^{2+} channel. In this study, in oocytes expressing WT-IQ channels, scoparone (EC_{50}, 5.54 μM) blocked CDI and promoted CDF of the Ca^{2+} channels and even caused slower inactivation of I_{Ca} than I_{Ba} (Fig. 6i; Fig. S16). However, in oocytes that expressed MT-AA channels and were pretreated with scoparone, CDI was quite robust (~78% increase in I_{Ba} compared to I_{Ca}, $p < 0.001$, Fig. 6i; Fig. S16). These results demonstrated that scoparone blocked CDI or promoted CDF of L-VGCC mediated by CaM by strengthening the CaM1-IQ interaction.

Discussion

Identifying novel targets of insecticides/acaricides with natural small molecules has been one of the greatest challenges in pest management [18,34,37]. In this study, RNA-seq was performed to screen candidate target genes by which scoparone acts against *T. cinnabarinus*. This method successfully identified Ca^{2+} signalling pathway genes; specifically, *TcL-, TcT-, TcN-VGCC* and *TcCaM1–5*, as candidate target genes for further research, opening new avenues for investigation of the modes of action of acaricides. Subsequently, the cDNA of these genes was cloned and verified, and the expression of these genes was knocked down by RNAi. Interestingly, simultaneous RNAi-mediated silencing of both L-VGCC and CaM1 reduced the sensitivity of *T. cinnabarinus* to scoparone much more strongly than silencing of each gene separately, suggesting that the mode of action of scoparone in mites involves overexpression of both the L-VGCC and CaM1 genes. It has been shown that L-VGCCs create potentials with long durations and slow inactivation that mediate the synaptic plasticity of neurons in the brain and are targeted by cardiovascular disease-treating drugs [23,28,38]. In addition, CaM, a principal Ca^{2+} sensor, regulates Ca^{2+} signalling by mediating the CDF and CDI of L-VGCC [28]. Thus, the novel Ca^{2+} signalling pathways mediated by CaM1 and L-VGCC are critical for the acaricidal mechanism of scoparone.

It can be hypothesized that the activation of Ca^{2+} signalling by scoparone is mediated by targeting and interaction with CaM1 and L-VGCC. The results of our series of *in vitro* and *in vivo* functional expression experiments, CaM assays, toxicity analyses, and $[Ca^{2+}]i$ assays support the above-described hypothesis. Previous research has suggested that CaM recovers Ca^{2+} channel activity during run-down in guinea pig cardiac myocytes (in an inside-out patch-clamp model) [39]. However, a channel-inactivating effect mediated by CaM has been found at high concentrations of CaM, suggesting that both facilitation and inactivation are mediated by CaM during run-down [29]. In intact myocytes, these CaM effects manifest as Ca^{2+}-dependent effects, indicating that these modes of action may emerge in CDF and CDI [28,39]. The relationship between CaM1 and scoparone in the modulation of L-VGCC was studied, and several novel findings were acquired. First, unlike CaM1, scoparone alone did not block Ca^{2+} channel activity at high concentrations (greater than10 μM). Second, the activating effect of scoparone on L-VGCCs was enhanced by CaM1. Third, the facilitatory and inhibitory effects of CaM1 were significantly enhanced and blocked by scoparone, respectively. These data strongly indicate that scoparone acts as an agonist of the CaM1 interaction with L-VGCC at the activation site.

How CaM binds to the several CaM-binding regions of channels mediating CDF and CDI and the specific types of CaM involved, has remained undetermined. Three regions of the C-terminus of L-VGCC, including the EF-hand, PreIQ and IQ regions, and the NT tail have been suggested to mediate CDF [40] and CDI [41,42]. Although the PreIQ and IQ motifs can bind CaM under high concentrations of Ca^{2+}, numerous studies have failed to measure CaM binding under low-Ca^{2+} conditions [43]. In addition, some reports have suggested that Ca^{2+}-insensitive CaM mutants bind very little to CT peptides [40,43] or IQ peptides [40]. In contrast, it has been reported that Ca^{2+} is not essential for CaM to bind to PreIQ [44] and IQ peptides [45]. Hence, whether CaM is tied to or structurally combines with the CT or NT region remains unclear. In this study, faint but identical binding of CaM to CT1 (at the near-end CT motif) under low-Ca^{2+} conditions (K_d ~ 0.931 μM) and very similar binding under high-Ca^{2+} conditions (K_d ~ 2.253/0.024 μM) were observed. The findings of electrophysiological experiments support this result: Ca^{2+} has been found to be indispensable for the channel-recovering effect of CaM, and the EC_{50} is higher under low-Ca^{2+} conditions than under high-Ca^{2+} conditions [39]. It can be hypothesized that CaM is not fixed to the Ca^{2+} channel but rather is dynamically bound to the channel on the basis of the CaM and Ca^{2+} levels [46]. Our results further support this hypothesis.

Knocking down the PreIQ [32,47], IQ [35,36,45] or EF-hand [35] regions of Ca^{2+} channels eliminates CDI mediated by CaM. Gel shift and fluorescence resonance energy transfer (FRET) assays have suggested that CaM competitively interacts with PreIQ and IQ peptides, which bind CaM at 1:1 stoichiometric ratios [29,35,43], indicating that one molecule of CaM mediates CDI by interacting with a site in the PreIQ or IQ region of the Ca^{2+} channel [48]. However, in this study, the results indicated that at least at high Ca^{2+} levels, multiple CaM molecules bind to the CT1B (PreIQ and IQ motifs) or CT1 peptide (EF-hand, PreIQ and IQ motifs). These results are consistent with prior crystallography [49,50] and thermokinetic

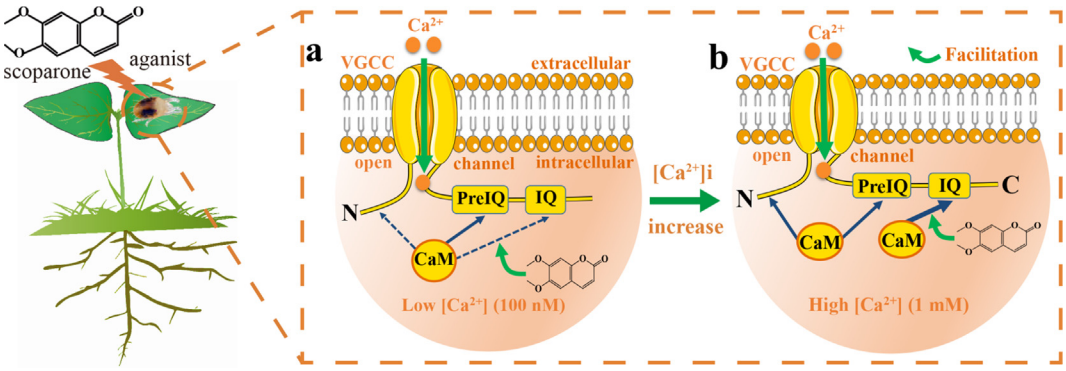

Fig. 7. Hypothetical model for the mechanism of action of scoparone against *T. cinnabarinus* via the CaM-mediated activation of L-VGCC. a At low [Ca^{2+}]i, CaM is mostly in the Ca^{2+}-free form (apoCaM) and interacts with elevated affinity with the PreIQ domain in the C-terminus of L-VGCC, producing basal channel activity. b However, as [Ca^{2+}]i increases, Ca^{2+}-bound CaM (Ca^{2+}/CaM) forms and interacts with elevated affinity with the IQ domain, resulting in CDF. Scoparone activates the CaM-binding site, which is located in the IQ region at the C-terminus of the Ca^{2+} channel. A further increase in [Ca^{2+}]i promotes the interaction of Ca^{2+}/CaM with PreIQ or the NT region, leading to CDI.

analyses [51]. There is little evidence supporting this scenario, but the discovery that scoparone facilitates CaM1 binding to the IQ motif is consistent with this hypothesis. Although CaM1 bound to a well-characterized IQ motif, mutations of the IQ motif that markedly weakened CaM1 binding blocked CDF and heightened CDI of Ca^{2+} channels during a single depolarizing pulse, suggesting that CaM interactions with the IQ motif actively suppressed inactivation or promoted facilitation of Ca^{2+} channels. Indeed, electrophysiological experiments confirmed these results, showing that scoparone did not promote CDF or block CDI in L-VGCC mutants (in which the combination of two key positions, Ile and Gln, in the IQ motif was replaced with Ala) because CaM1 binding to the IQ region of the Ca^{2+} channel was impaired.

Notably, it has been reported that CaM binds to the N-termini of Ca^{2+} channels [36], which was confirmed in this study. However, the affinity of PreIQ (K_d ~ 0.085 μM) for CaM was much higher than that of the NT region (K_d ~ 0.112 μM), indicating that the NT region cannot be the CaM-interacting site that triggers the basal activity of Ca^{2+} channels. In contrast, it can be reasonably hypothesized that the NT region acts as a CaM-binding site mediating CDI [36] and that both the NT and CT motifs may interact with CaM to result in CDI.

According to the current findings, it can be hypothesized that the mode of action of scoparone involves CaM-mediated Ca^{2+} channels (Fig. 7). At low [Ca^{2+}]i, CaM exists mainly in a Ca^{2+}-free form (apoCaM) and interacts with relatively high affinity with PreIQ (a CT motif of Ca^{2+} channels), producing basal channel activity. Due to the relatively low affinity of apoCaM for the IQ/NT region, the interaction between them may be minimal [52]. However, when [Ca^{2+}]i increases, Ca^{2+} binds with CaM, forming Ca^{2+}/CaM, which binds with relatively high affinity to the IQ motif, triggering CDF. Scoparone induces Ca^{2+}/CaM binding at this site as an agonist, after which Ca^{2+} channel activity is induced in a concentration-dependent manner. Further increases in [Ca^{2+}]i enhance the binding of Ca^{2+}/CaM with PreIQ/NT, leading to CDI. This model explains how mid-range [Ca^{2+}]i mediates CDF, while elevated [Ca^{2+}]i mediates CDI.

Conclusion

This study suggests that the mode of action of scoparone involves targeting of the interface between CaM1 and L-VGCC and modulation of the downstream Ca^{2+} signalling pathways. Interestingly, CaM enhances the channel-activating effects of scoparone. Scoparone activates the CaM-binding site, which is located in the IQ motif at the Ca^{2+} channel C-terminus. Thus, the IQ motif may be a promising novel "green acaricide"-binding target site of scoparone. Its identification may accelerate the development of novel acaricides to control destructive phytophagous pest mites worldwide. Furthermore, the findings of this study may contribute to the development of target-specific green acaricidal compounds based on L-VGCC.

Compliance with Ethics Requirements

This article does not contain any studies with human or animal subjects.

Declaration of Competing Interest

The authors declare that they have no known competing financial interests or personal relationships that could have appeared to influence the work reported in this paper.

Acknowledgements

Research was supported by grant from the National Science Foundation of China (31972288) and the Innovation Fund for Graduate Students of Chongqing (CYB21118).

Appendix A. Supplementary data

Supplementary data to this article can be found online at https://doi.org/10.1016/j.jare.2021.08.013.

References

[1] Grbić M, Leeuwen TV, Clark RM, Rombauts S, Rouze P, Grbic V, et al. The genome of Tetranychus urticae reveals herbivorous pest adaptations. Nature 2011;479:487–92. doi: https://doi.org/10.1038/nature10640.
[2] Feng K, Liu J, Wei P, Ou S, Wen X, Shen G, et al. lincRNA_Tc13743. 2-miR-133-5p-TcGSTm02 regulation pathway mediates cyflumetofen resistance in Tetranychus cinnabarinus. Insect Biochem. Mol. Biol. 2020;123:103413. doi: https://doi.org/10.1016/j.ibmb.2020.103413.
[3] Gould F, Brown ZS, Kuzma J. Wicked evolution: Can we address the sociobiological dilemma of pesticide resistance?. Science 2018;360:728–32. doi: https://doi.org/10.1126/science.aar3780.
[4] Chen L, Sun JT, Jin PY, Hoffmann AA, Bing XL, Zhao DS, et al. Population genomic data in spider mites point to a role for local adaptation in shaping range shifts. Evol. Appl. 2020;13:2821–35. doi: https://doi.org/10.1111/eva.13086.
[5] Xu S, Zeng X, Dai S, Wang J, Chen Y, Song J, et al. Turpentine Derived Secondary Amines for Sustainable Crop Protection: Synthesis, Activity Evaluation and QSAR Study. J Agric Food Chem 2020;68:11829–38. doi: https://doi.org/10.1021/acs.jafc.0c01909.
[6] Shang X-F, Dai L-X, Yang C-J, Guo X, Liu Y-Q, Miao X-L, et al. A value-added application of eugenol as acaricidal agent: The mechanism of action and the

safety evaluation. J. Adv. Res. 2020. doi: https://doi.org/10.1016/j.jare.2020.12.010.
[7] Kim JK, Kim JY, Kim HJ, Park KG, Harris RA, Cho WJ, et al. Scoparone Exerts Anti-Tumor Activity against DU145 Prostate Cancer Cells via Inhibition of STAT3 Activity. PLoS ONE 2013;8:. doi: https://doi.org/10.1371/journal.pone.0080391e80391.
[8] Fang H, Zhang A, Yu J, Wang L, Liu C, Zhou X, et al. Insight into the metabolic mechanism of scoparone on biomarkers for inhibiting Yanghuang syndrome. Sci Rep 2016;6:37519. doi: https://doi.org/10.1038/srep37519.
[9] Choi YH, Yan GH. Anti-allergic effects of scoparone on mast cell-mediated allergy model. Phytomedicine 2009;16:1089–94. doi: https://doi.org/10.1016/j.phymed.2009.05.003.
[10] Jang SI, Kim YJ, Lee WY, Kwak KC, Baek SH, Kwak GB, et al. Scoparone from *Artemisia capillaris* inhibits the release of inflammatory mediators in RAW 264.7 cells upon stimulation cells by interferon-gamma Plus LPS. Arch. Pharm. Res. 2005;28:203–8. doi: https://doi.org/10.1007/BF02977716.
[11] Hou QL, Luo JX, Zhang BC, Jiang GF, Ding W, Zhang YQ. 3D-QSAR and Molecular Docking Studies on the *TcPMCA1*-Mediated Detoxification of Scopoletin and Coumarin Derivatives. Int J Mol Sci 2017;18:1380. doi: https://doi.org/10.3390/ijms18071380.
[12] Luo J, Lai T, Guo T, Chen F, Zhang L, Ding W, et al. Synthesis and Acaricidal Activities of Scopoletin Phenolic Ether Derivatives: QSAR. Molecular Docking Study and in Silico ADME Predictions, Molecules 2018;23:995. doi: https://doi.org/10.3390/molecules23050995.
[13] Zhou H, Liu J, Wan F, Guo F, Ning Y, Liu S, et al. Insight into the mechanism of action of scoparone inhibiting egg development of *Tetranychus cinnabarinus* Boisduval. Comp. Biochem. Phys. C 2021;246:. doi: https://doi.org/10.1016/j.cbpc.2021.109055109055.
[14] Huang X, Lv M, Xu H. Semisynthesis of novel N-acyl/sulfonyl derivatives of 5 (3,5)-(di)halogenocytisines/cytisine and their pesticidal activities against *Mythimna separata* Walker, *Tetranychus cinnabarinus* Boisduval, and *Sitobion avenae* Fabricius. Pest Manag Sci 2019;75:2598–609. doi: https://doi.org/10.1002/ps.5375.
[15] Ma S, Liu J, Lu X, Zhang X, Ma Z. Effect of Wilforine on the Calcium Signaling Pathway in *Mythimna Separata* Walker Myocytes Using Calcium Imaging Technique. J Agric Food Chem 2019;67:13751–7. doi: https://doi.org/10.1021/acs.jafc.9b05592.
[16] Marchi S, Patergnani S, Missiroli S, Morciano G, Rimessi A, Wieckowski MR, et al. Mitochondrial and endoplasmic reticulum calcium homeostasis and cell death. Cell Calcium 2018;69:62–72. doi: https://doi.org/10.1016/j.ceca.2017.05.003.
[17] Xu T, Yuchi ZG. Crystal structure of diamondback moth ryanodine receptor Repeat34 domain reveals insect-specific phosphorylation sites. BMC Biol 2019;17:77. doi: https://doi.org/10.1186/s12915-019-0698-5.
[18] Ma R, Haji-Ghassemi O, Ma D, Jiang H, Lin L, Li Y, et al. Structural basis for diamide modulation of ryanodine receptor. Nat. Chem. Biol. 2020;16:1246–54. doi: https://doi.org/10.1038/s41589-020-0627-5.
[19] Ma X, Zhang Y, Guo F, Luo J, Ding W, Zhang Y. Molecular characterization of a voltage-gated calcium channel and its potential role in the acaricidal action of scopoletin against *Tetranychus cinnabarinus*. Pestic Biochem Physiol 2020;168:. doi: https://doi.org/10.1016/j.pestbp.2020.104618104618.
[20] Zhou H, Zhang Y, Lai T, Liu X, Guo F, Guo T, et al. Acaricidal Mechanism of Scopoletin Against *Tetranychus cinnabarinus*. Front Physiol 2019;10:164. doi: https://doi.org/10.3389/fphys.2019.00164.
[21] Blum ID, Keleş MF, Baz E-S, Han E, Park K, Luu S, et al. Astroglial Calcium Signaling Encodes Sleep Need in Drosophila. Curr. Biol. 2021;31:150–62. doi: https://doi.org/10.1016/j.cub.2020.10.012.
[22] Fu S, Yang L, Li P, Hofmann O, Dicker L, Hide W, et al. Aberrant lipid metabolism disrupts calcium homeostasis causing liver endoplasmic reticulum stress in obesity. Nature 2011;473:528–31. doi: https://doi.org/10.1038/nature09968.
[23] Atsuta Y, Tomizawa RR, Levin M, Tabin CJ. L-type voltage-gated Ca2+ channel CaV1.2 regulates chondrogenesis during limb development. Proc. Natl. Acad. Sci. U. S. A. 2019;116:21592–601. doi: https://doi.org/10.1073/pnas.1908981116.
[24] Dyla M, Kjærgaard M, Poulsen H, Nissen P. Structure and Mechanism of P-Type ATPase Ion Pumps. Annu. Rev. Biochem. 2020;89:583–603. doi: https://doi.org/10.1146/annurev-biochem-010611-112801.
[25] Gong D, Chi X, Wei J, Zhou G, Huang G, Zhang L, et al. Modulation of cardiac ryanodine receptor 2 by calmodulin. Nature 2019;572:347–51. doi: https://doi.org/10.1126/science.aat7744.
[26] Steven JL, Thao PT, Que TN, Vera Y-M-B, Wah C, Irina IS. Flexible Architecture of IP_3R_1 by Cryo-EM. Cell 2011;19:1192–9. doi: https://doi.org/10.1016/j.str.2011.05.003.
[27] Yang YJ, Lee HJ, Lee BK, Lim SC, Chong KL, Lee MK. Effects of scoparone on dopamine release in PC12 cells. Fitoterapia 2010;81:497–502. doi: https://doi.org/10.1016/j.fitote.2010.01.00.
[28] Dixon RE, Moreno CM, Yuan C, Opitz-Araya X, Binder MD, Navedo MF, et al. Graded Ca2+/calmodulin-dependent coupling of voltage-gated CaV1.2 channels. eLife 2015;4:e05608. doi: https://doi.org/10.7554/eLife.05608.
[29] Xiong L, Kleerekoper QK, He R, Putkey JA, Hamilton SL. Sites on calmodulin that interact with the C-terminal tail of Cav1.2 channel. J. Biol. Chem. 2005;280:7070–9. doi: https://doi.org/10.1074/jbc.M410558200.
[30] Zhou H, Guo F, Luo J, Zhang Y, Liu J, Zhang Y, et al. Functional analysis of an upregulated calmodulin gene related to the acaricidal activity of curcumin against Tetranychus cinnabarinus (Boisduval). Pest Manag. Sci. 2021;77:719–30. doi: https://doi.org/10.1002/ps.6066.
[31] Shen XM, Liao CY, Lu XP, Zhe W, Wang JJ, Wei D. Involvement of Three Esterase Genes from *Panonychus citri* (McGregor) in Fenpropathrin Resistance. Int J Mol Sci 2016;17:1–15. doi: https://doi.org/10.3390/ijms17081361.
[32] Etsuko M, Hadhimulya A, Saud ZA, Masaki K. Calpastatin domain L is a partial agonist of the calmodulin-binding site for channel activation in Cav1.2 Ca2+ channels. J. Biol. Chem. 2011;286:39013–22. doi: https://doi.org/10.1074/jbc.M111.242248.
[33] Chen Z, Yao X, Dong F, Duan H, Shao X, Chen X, et al. Ecological toxicity reduction of dinotefuran to honeybee: New perspective from an enantiomeric level. Environ Int 2019;130:1–8. doi: https://doi.org/10.1016/j.envint.2019.05.048.
[34] Xu Z, Hu Y, Hu J, Qi C, Zhang M, Xu Q, et al. The interaction between abamectin and RDL in the carmine spider mite: a target site and resistant mechanism study. Pestic. Biochem. Physiol. 2020;164:191–5. doi: https://doi.org/10.1016/j.pestbp.2020.01.010.
[35] Zühlke RD, Pitt GS, Tsien RW, Reuter H. Ca2+-sensitive inactivation and facilitation of L-type Ca2+ channels both depend on specific amino acid residues in a consensus calmodulin-binding motif in the α1C subunit. J. Biol. Chem. 2000;275:21121–9. doi: https://doi.org/10.1074/jbc.M002986200.
[36] Zhou H, Yu K, McCoy KL, Lee A. Molecular Mechanism for Divergent Regulation of Cav1.2 Ca2+ Channels by Calmodulin and Ca2+-binding Protein-1. J. Biol. Chem. 2005;280:29612–9. doi: https://doi.org/10.1074/jbc.M504167200.
[37] Sun Z, Lv M, Yu X, Xu H. Application of Sustainable Natural Bioesources in Crop Protection: Insight into a Podophyllotoxin-Derived Botanical Pesticide for Regulating Insect Vestigial Wing of *Mythimna separata* Walker. ACS Sustain. Chem. Eng. 2017;5:3945–54. doi: https://doi.org/10.1021/acssuschemeng.6b03145.
[38] Catterall WA, Lenaeus MJ, El-Din TMG. Structure and Pharmacology of Voltage-Gated Sodium and Calcium Channels. Annu. Rev. Pharmacol. Toxicol. 2020;60:133–54. doi: https://doi.org/10.1146/annurev-pharmtox-010818-021757.
[39] Han DY, Minobe E, Wang W-Y, Guo F, Xu J-J, Hao L-Y, et al. Calmodulin- and Ca2+-Dependent Facilitation and Inactivation of the CaV1.2 Ca2+ Channels in Guinea-Pig Ventricular Myocytes. J. Pharmacol. Sci. 2010;112:310–9. doi: https://doi.org/10.1254/jphs.09282FP.
[40] Badone B, Ronchi C, Kotta MC, Sala L, Ghidoni A, Crotti L, et al. Calmodulinopathy: Functional Effects of CALM Mutations and Their Relationship With Clinical Phenotypes. Front. Cardiovasc. Med. 2018;5:176. doi: https://doi.org/10.3389/fcvm.2018.00176.
[41] Barrett CF, Tsien RW. The Timothy syndrome mutation differentially affects voltage- and calcium-dependent inactivation of CaV1.2 L-type calcium channels. Proc. Natl. Acad. Sci. U. S. A. 2008;105:2157–62. doi: https://doi.org/10.1073/pnas.0710501105.
[42] Abderemane-Ali F, Findeisen F, Rossen ND, Minor DL. A Selectivity Filter Gate Controls Voltage-Gated Calcium Channel Calcium-Dependent Inactivation. Neuron 2019;101:1134–49. doi: https://doi.org/10.1016/j.neuron.2019.01.011.
[43] Pitt ES et al. Molecular Basis of Calmodulin Tethering and Ca2+-dependent Inactivation of L-type Ca2+ Channels. J. Biol. Chem. 2001;276:30794–802. doi: https://doi.org/10.1074/jbc.M104959200.
[44] Kepplinger KJF, Forstner G, Kahr H, Leitner K, Pammer P, Groschner K, et al. Molecular determinant for run-down of L-type Ca2+ channels localized in the carboxyl terminus of the α1C subunit. J. Physiol. 2000;529:119–30. doi: https://doi.org/10.1111/j.1469-7793.2000.00119.x.
[45] Wang KQ, Holt C, Lu J, Brohus M, Larsen KT, Overgaard MT, et al. Arrhythmia mutations in calmodulin cause conformational changes that affect interactions with the cardiac voltage-gated calcium channel. Proc. Natl. Acad. Sci. U. S. A. 2018;115:E10556–65. doi: https://doi.org/10.1073/pnas.1808733115.
[46] Asmara H, Minobe E, Saud ZA, Kameyama M. Interactions of Calmodulin With the Multiple Binding Sites of Cav 1.2 Ca2+ Channels. J. Pharmacol. Sci. 2010;112:397–404. doi: https://doi.org/10.1254/jphs.09342FP.
[47] Findeisen F, Tolia A, Arant R, Young Kim E, Isacoff E, Minor JDL. Calmodulin overexpression does not alter Cav1.2 function or oligomerization state. Channels, 5. p. 320–4. doi: https://doi.org/10.4161/chan.5.4.16821.
[48] Mori MX, Erickson MG, Yue DT. Functional Stoichiometry and Local Enrichment of Calmodulin Interacting with Ca^{2+} Channels. Science 2004;304:432–5. doi: https://doi.org/10.1126/science.1093490.
[49] Kim EY, Rumpf CH, Petegem FV, Arant RJ, Findeisen F, Cooley ES, et al. Multiple C-terminal tail Ca2+/CaMs regulate CaV 1.2 function but do not mediate channel dimerization. EMBO J. 2010;29:3924–38. doi: https://doi.org/10.1038/emboj.2010.277.
[50] Fallon JL, Baker MR, Xiong L, Loy RE, Yang G, Dirksend RT, et al. Crystal structure of dimeric cardiac L-type calcium channel regulatory domains bridged by Ca^{2+}/calmodulins. Proc. Natl. Acad. Sci. U. S. A. 2008;106:5135–40. doi: https://doi.org/10.1073/pnas.0807487106.
[51] Evans TIA, Hell J, She MA. Thermodynamic linkage between calmodulin domains binding calcium and contiguous sites in the C-terminal tail of CaV 1.2. Biophys. Chem. 2011;159:172–87. doi: https://doi.org/10.1016/j.bpc.2011.06.007.
[52] Banerjee R, Yoder JB, Yue DT, Amzel LM, Tomaselli GF, Gabelli SB, et al. Bilobal architecture is a requirement for calmodulin signaling to $Ca_V1.3$ channels. Proc. Natl. Acad. Sci. U. S. A. 2018;115:E3026–35. doi: https://doi.org/10.1073/pnas.1716381115.